Vehicle Dynamics in Pickup-And-Delivery Problems Using Electric Vehicles

Saman Ahmadi[1] ✉ 📵
Department of Data Science and AI, Monash University, Victoria, Australia
CSIRO Data61, Canberra, Australia

Guido Tack ✉
Department of Data Science and AI, Monash University, Victoria, Australia

Daniel Harabor ✉
Department of Data Science and AI, Monash University, Victoria, Australia

Philip Kilby ✉
CSIRO Data61, Canberra, Australia

─── **Abstract** ───

Electric Vehicles (EVs) are set to replace vehicles based on internal combustion engines. Path planning and vehicle routing for EVs need to take their specific characteristics into account, such as reduced range, long charging times, and energy recuperation. This paper investigates the importance of vehicle dynamics parameters in energy models for EV routing, particularly in the Pickup-and-Delivery Problem (PDP). We use Constraint Programming (CP) technology to develop a complete PDP model with different charger technologies. We adapt realistic instances that consider vehicle dynamics parameters such as vehicle mass, road gradient and driving speed to varying degrees. The results of our experiments show that neglecting such fundamental vehicle dynamics parameters can affect the feasibility of planned routes for EVs, and fewer/shorter charging visits will be planned if we use energy-efficient paths instead of conventional shortest paths in the underlying system model.

1 Introduction

The Pickup-and-Delivery Problem (PDP) is a well-studied problem in Constraint Programming (CP) and Operations Research. PDP is a point-to-point transport problem where a fleet of vehicles needs to serve requests for moving loads/passengers between a set of pickup and delivery points. In this problem, transit requests are known and vehicles can start and terminate their trips at particular depots. The solution to the PDP is a set of routes (one route per vehicle) that satisfies both problem objectives (e.g. shortest tours) and transport constraints (such as time windows and energy requirements).

In this study, we are interested in the PDP using Electric Vehicles (EVs). The electrification of transport systems is a well-known and efficient practice to reduce transport emissions. Compared to the conventional combustion-based vehicles, battery-powered vehicles are less

---

[1] Corresponding Author

dependant on fossil sources and offer higher energy efficiencies. However, limited driving range and the lengthy charging process in EVs may require substantially different routing decisions compared to conventional vehicles. As an example, in cases where the EV's available energy is not sufficient to plan point-to-point trips, charging detours need to be considered. Hence, the transport model needs to carefully track the EVs' energy levels to ensure the feasibility of planned trips by possibly adding necessary charging stops.

In transport systems with EVs, energy matters can generally be studied from two aspects: energy absorbed at charging points and energy consumed in point-to-point trips (discharging). Depending on the required energy and also the technology used at charging points, charging times may vary from a few minutes to several hours. A common practice to model the charging component of the transport system is establishing a linear relationship between energy and time [8, 16]. However, as EV chargers can adapt their power with the battery's remaining energy (slower charging rate in higher state of charge), linear charging models may not be able to correctly reflect the actual charging time needed for a specific amount of energy. To address this inaccuracy, recent studies have employed more realistic charging profiles for their transport models to accommodate various charging technology types via piece-wise linear approximations [15, 13].

Discharging (while driving) is the other aspect of energy matters in EVs. Similar to charging, transport models require an energy model that appropriately accounts for energy consumption. A common (but inaccurate) method to estimate the energy consumption of point-to-point trips is to use a fixed energy consumption rate (measuring units of energy per unit of distance/time) [11, 19]. This means that basic models assume shortest/fastest point-to-point paths to also be the most energy-efficient paths. However, there are several important parameters in vehicle dynamics that are ignored in linear consumption models, such as driving patterns, vehicle mass and road gradients. Therefore, the estimated energy costs obtained by using basic models are not accurate and there is always a high risk for planned trips to be infeasible in reality. Due to the complexity of realistically estimating the discharging energy in EVs, attempts to add some parameters of vehicle dynamics into energy models may lead to major simplifications in the energy model such as ignoring vehicle acceleration or neglecting changes in ground slope [9].

To better explain to what extent vehicle dynamics can affect the energy consumption in EVs, we solved a PDP with 14 transport demands in San Francisco as depicted in Figure 1 (Right). The trip was planned using the average (fixed rate) energy consumption of the *Peugeot iOn* as an EV with 16 kWh battery capacity and 100% initial energy level. As shown in Figure 1, the EV can transport all of the passengers to their destination using less than 100% of the energy capacity (red line). Therefore, the planned trip seems feasible with the basic (fixed-rate) energy model. But the situation changes when we recalculate the energy requirement of the planned multi-stop trip via three other energy models that take vehicle dynamics into account to varying degrees. As seen in Figure 1 (Left), the trip would require more energy when passenger weights are included (blue line). Energy consumption further increases when the ground slope is added into the energy calculation (green and yellow curves), making the last two pickups (at a distance of 120km) infeasible with more accurate energy models. Therefore, given the fact that trips can be planned for every possible initial energy level, neglecting vehicle dynamics parameters can potentially result in infeasible trips.

This paper investigates the implications of adding vehicle dynamics into the EV route planning. To this end, we establish an energy-based PDP transport model that can handle realistic charging and discharging profiles of EVs. We use CP technology to prototype a solver for the PDP that can deal with the new transport model. This allows us to conduct a
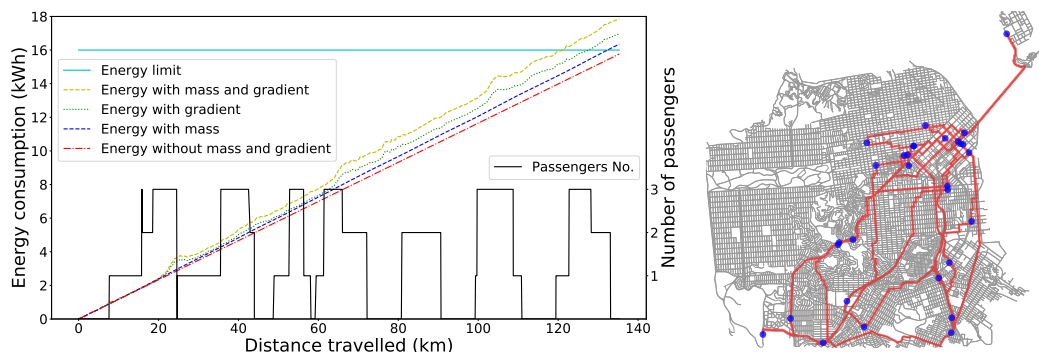
Figure 1 [Coloured] Right: A Sample multi-stop trip in San Francisco, Left: Pickup and drop-off of passengers during the trip, also energy requirement of the trip using different energy models versus the distance travelled.

detailed study of the new model and evaluate it with a new set of realistic instances that accounts for challenging requirements of EV energy models in two scenarios: using shortest or energy-efficient point-to-point paths. The results of our experimental study show that it is crucial to use more accurate transport models to avoid the risk of seriously underestimating energy requirements. These results justify an investment into new solving technology that can handle these accurate models efficiently.

2   Energy Consumption Models

When solving routing problems for EVs, the energy requirement of the underlying point-to-point paths are determined based on an *energy model*, which determines how much energy the vehicle will consume (or indeed recuperate) when travelling from point A to point B. Energy models can differ dramatically in their complexity. A very basic model may estimate energy requirements over a path long length d by simply using an average energy consumption rate β (in Wh/100m), resulting in the simple equation $E = \beta \times d$. This simplistic energy model provides a rough approximation and does not fully take into account the main parameters in vehicle dynamics, such as road gradient, vehicle mass or acceleration. To better understand the importance of the vehicle dynamics parameters, Figure 2 (Right) shows changes in energy efficiency with different road gradients and extra mass for the *Peugeot iOn* as a test EV with an initial energy level of 70%. We use the realistic WLTP drive cycle[2] depicted in Figure 2 (Left). We see a slight but clear non-linear relationship between energy efficiency and road gradient. Furthermore, the figure shows that increasing vehicle mass can either increase or decrease energy efficiency depending on the gradient.

In positive gradients, the energy requirement of links increases with mass, but this is not always the case in negative gradients. EVs can potentially recover part of the kinetic energy via regenerative braking. This means that energy consumption can even be negative on negative slopes as shown in Figure 2 (Right). If the energy requirement of a link is negative (on negative slopes), increasing mass would contribute to recuperating more energy and, therefore, decreased energy consumption. Figure 2 (Right) also highlights that the amount of energy the EV can regenerate on a negative slope is much less than the energy it needs to climb up the same gradient. This difference is mainly due to the total powertrain efficiency and hybrid (mechanical+electric) braking strategy in EVs.

---

[2]   Worldwide Harmonised Light Vehicles Test Procedure
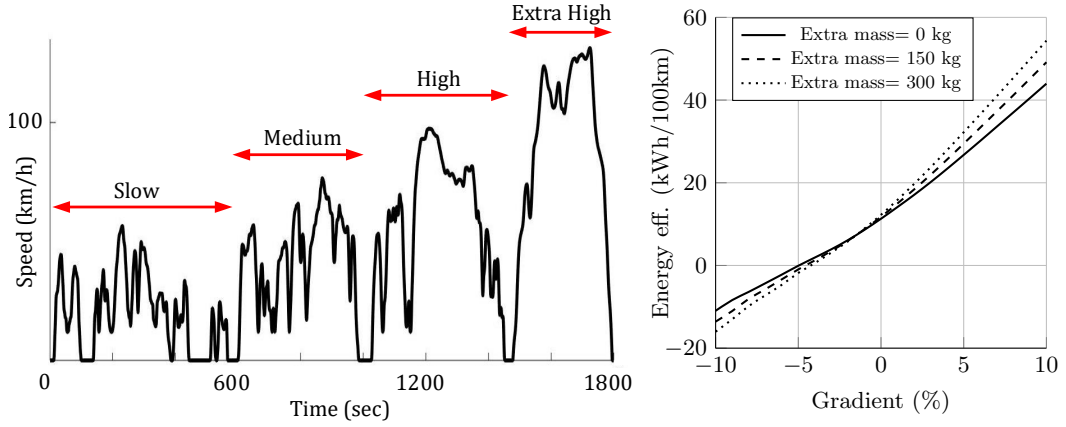
Figure 2 Left: Speed profiles in the WLTP cycle, Right: Energy efficiency vs. gradient and extra mass over WLTP for the *Peugeot iOn* with the average energy efficiency of 11.6 kWh/100km.

As the exact calculation of the links' energy requirement in the PDP setting is a difficult task, we build our energy models based on three main parameters in vehicle dynamics that change with transport request/location. These parameters are gradient, speed profiles (acceleration/deceleration) and extra mass. In this study, we investigate six different energy models. Our most accurate energy model is given in Eq. (1). We call this full model E_{gv}^m, since it takes gradient g, speed profiles v and extra mass m into account.

$$E_{gv}^m = \left((\alpha_{1,i}m + \beta_{1,i})g^2 + (\alpha_{2,i}m + \beta_{2,i})g + (\alpha_{3,i}m + \beta_{3,i}) \right) d \tag{1}$$

In Eq. (1), E_{gv}^m is the energy requirement (in Wh), g is the road angle ($\sin\theta$), d is the link distance (in units of 100m) and m is the extra mass (load/passenger weights in kg). Coefficients α_i (in Wh/(100m*kg)) and β_i (in Wh/100m) are parameters that depend on the selected speed profile i and also vehicle specification. These coefficients can be obtained using the relationship depicted in Figure 2 (Right) for every EV evaluated under a driving pattern. Table 1 shows α_i and β_i values for our test EV *Peugeot iOn* simulated under the speed profiles of the WLTP driving cycle (Slow, Medium, High, Extra-High) after fitting a polynomial of degree two to the operating points obtained for each speed profile (see Figure 2 (Left) for the overall WLTP pattern). We define the energy requirement of a path to be the aggregation of the energy requirements of all of its links.

We first define our *basic energy model* to be the model that just uses the EV's average energy efficiency, i.e. $E_b = \beta_3 d$. If extra mass is to be considered in the basic model, we then have $E_b^m = (\alpha_3 m + \beta_3)d$. Our second model incorporates road gradient g as an additional parameter via $E_g = (\beta_1 g^2 + \beta_2 g + \beta_3)d$. Analogously, adding extra mass to this model yields $E_g^m = ((\alpha_1 m + \beta_1)g^2 + (\alpha_2 m + \beta_2)g + (\alpha_3 m + \beta_3))d$. Given the nonlinear relationship in Figure 2 (Right) for every driving pattern, our last case accounts for both gradient g and speed v impacts on energy consumption via $E_{gv} = (\beta_{1,i}g^2 + \beta_{2,i}g + \beta_{3,i})d$. Finally, adding mass to this model yields our full energy model E_{gv}^m as in Eq. (1). Table 2 shows a summary of our energy models with and without extra mass consideration. Note that for the models with a fixed speed profile such as E_b and E_g, we use the average energy coefficients obtained for the concrete WLTP drive cycle (last profile in Table 1).

Table 1 Energy specification and coefficients of the *Peugeot iOn* based on the profiles in WLTP. α in Wh/(100m*kg) and β in Wh/100m.

Vehicle details	Profile	α_1	α_2	α_3	β_1	β_2	β_3
Peugeot iOn 2017	Slow	0.398	0.244	0.005	315.33	264.69	12.60
Capacity: 16 kWh	Medium	0.451	0.241	0.004	381.85	262.25	10.04
Efficiency*: $\sim$11.6 $\frac{Wh}{100m}$	High	0.526	0.249	0.004	511.05	259.70	10.36
Kerb weight: 1050 kg	Extra High	0.731	0.262	0.004	734.48	293.05	13.31
	Overall (avg.)	0.579	0.251	0.004	536.72	272.77	11.65

Table 2 Summary of energy models versus parameters of vehicle dynamics.

Model	Parameters	Without Mass	Adding Mass (m)
E_b	-	$\beta_3 d$	$+ m\alpha_3 d$
E_g	gradient	$(\beta_1 g^2 + \beta_2 g + \beta_3)d$	$+ m(\alpha_1 g^2 + \alpha_2 g + \alpha_3)d$
E_{gv}	gradient, speed	$(\beta_{1,i} g^2 + \beta_{2,i} g + \beta_{3,i})d$	$+ m(\alpha_{1,i} g^2 + \alpha_{2,i} g + \alpha_{3,i})d$

3 EV Routing Problem

This section explores the impacts of vehicle dynamics on the PDP when EVs are operated in the transport system. In this problem, EVs start and terminate trips at particular depots and transit requests are known in advance. A solution to this PDP is a set of routes (one route per vehicle) that satisfies both problem objectives (e.g. fastest/shortest tours) and fundamental constraints such as passenger time windows [18]. Furthermore, there are other considerations such as tracking the EVs' energy levels and charging times to ensure route feasibility.

The PDP model for EVs should respect the correlations between energy matters in EVs and routing constraints in the PDP. Although Mixed-Integer Programming (MIP) is a traditional modelling approach in routing problems, in this study, we use CP to design and develop our PDP model as it provides a greater degree of flexibility in the way our non-linear energy constraints are handled. For this purpose, we develop our energy-based PDP model in MiniZinc [14].

We define each possible origin/destination location in our model to be a node with at most one status from N={*pickup, drop-off, depot, charger*}. This means that we model every transport request with a *(pickup,drop-off)* pair, each EV initially at a *depot* node, and each charger with at least one *charger* node per visit (multiple nodes if more than one visit is allowed). For the CP model of this study, we use the *Successor* representation to encode the EVs' trips. We explain this approach using an example shown in Figure 3. For the simple trip planned in Figure 3 (Left) and the nodes' successors (Right), we can execute the full trip by sequentially looking up each node's successor to obtain the sequence {1-3-2-5-1}, given node 1 as the depot. Node 4 is not part of the trip.

Problem objective. Following the traditional objective definition in vehicle routing problems, we aim to plan routes that are optimal in terms of total travel time, i.e., in the context of EVs, our objective is minimising both the travel time and charging time.
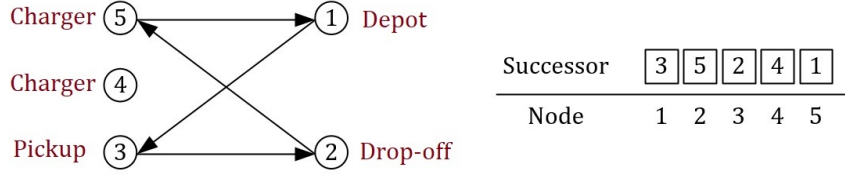
■ **Figure 3** Left: An example trip for the successor representation, Right: *Successor* array.

3.1   PDP Constraints

The essential step in the PDP is keeping track of the (non-negative) trip time t at non-charger nodes by

$$t[j] \geq t[i] + t_s[i] + \Delta t[i,j] \qquad i \in N - \{charger\} \quad \text{and} \quad j = succ[i] \tag{2}$$

The constraint above ensures that the service time t_s of non-charger node i and also the time required to reach $succ[i]$ from node i is preserved in the trip time when the EV arrives at $succ[i]$. We assume the point-to-point travel time matrix Δt has already been pre-computed and is available as input to our model. In addition, we consider a constant service time for every node in our model (zero for depot).

In PDP with time windows, we also need to make sure that the arrival times are always within the time limit of the transport demands, i.e, for every *pickup* node we have

$$t_{low}[i] \leq t[i] \leq t_{up}[i] \qquad i \in pickup \tag{3}$$

where t_{low} and t_{up} are the lower and upper time limits of pickup nodes respectively. In order to prevent long trips for every individual transport request, we limit the the travel time for transport requests by

$$0 \leq t[j] - t[i] \leq \lambda \times \Delta t[i,j] \qquad (i,j) \in (pickup, dropoff) \tag{4}$$

where $\lambda > 1$ is a constant factor that scales the time required to traverse the direct route between pickup and drop-off nodes. For example, setting $\lambda = 2$ means that the total time each transport request spends in our EV is at most two times longer than its direct route. The constraint above also makes sure that drop-off occurs after pickup.

Respecting the vehicle capacity is another essential step in PDP system models. That is, given the vehicle capacity C, we need to make sure that the EV transfers at most C passengers in every point-to-point trip:

$$0 \leq u[i] \leq C \qquad i \in N \tag{5}$$

where the variable $u[i]$ represents the vehicle utilisation (number of passengers) when the EV departs from node i. Meanwhile, in order to accurately track the EVs' loads, we have

$$u[j] = u[i] + \Delta u[j] \qquad i \in N \quad \text{and} \quad j = succ[i] \tag{6}$$

where $\Delta u[j]$ indicates the utilisation change at the successor node j (the node that will be visited after node i in the trip). The value of Δu is positive at pickup nodes, negative at drop-offs and zero at other nodes. Note that since this parameter will be part of our energy calculations, we use equality (=) in the constraint above to always have the exact utilisation value (and more accurate energy estimates respectively) at departure. Similar to

the point-to-point travel time array Δt, the Δu array is pre-computed using the problem specification. We can also add a constraint for vehicle utilisation at charger points. If we do not want to have any passenger on board while charging, we simply set

$$u[i] = 0 \qquad i \in charger \tag{7}$$

As an extra constraint, we use the global CP constraint `subcircuit` to create a set of circuits (trips) through our *Successor* array. Since visiting all charging points is not necessary, this constraint allows us to plan trips without charging visits. Figure 4 (Right) depicts sample solution tours using this constraint when EVs are allowed to return to any of the depots.

3.2   Energy Constraints

We now present energy constraints needed for appropriate energy tracking in the PDP for EVs. We again use the trip sequence available in the *Successor* array for our energy tracking approach. For every *demand* node, the available energy of the EV at its successor node is estimated using the following constraint.

$$e[j] = e[i] - \Delta e[i, j, k] \qquad i \in \{pickup, dropoff\} \quad \text{and} \quad j = succ[i] \quad \text{and} \quad k = u[i] \tag{8}$$

Where $e[j]$ is the arrival energy level at successor node j and the 3-dimensional array Δe represents the energy requirement of traversing the path between a demand location i and its successor $succ[i]$, with $u[i]$ passengers in the EV. Similarly, for the *depot* nodes we track energy consumption by

$$e[j] = e_{init}[i] - \Delta e[i, j, k] \qquad i \in depot \quad \text{and} \quad j = succ[i] \quad \text{and} \quad k = u[i] \tag{9}$$

where $e_{init}[i]$ is the initial energy level of our EVs at their designated depot node i (zero for non-depot nodes). Furthermore, as charging time depends on the available energy at nodes, we use equality ($=$) in the constraints above to always have the exact energy values for our charging time calculations. In other words, by using equality, we do not allow the model to set arbitrarily low arrival energy values to benefit from higher charging rates (in lower energy levels) and consequently shorter charge times. It is worth mentioning that we define the range of our energy-based decision variables to be $[0, E]$ where E is the energy capacity of the EV. This means critical cases (running out of energy and overcharging) are already considered in our CP model, i.e., for every node i we have $0 \le e[i] \le E$.

We can see that adding mass (vehicle utilisation) to the PDP model increases the system complexity, since the number of passengers in the vehicle at any location is a decision variable, and therefore the energy requirement Δe may no longer be constant, depending on whether the energy model does take mass into account. Nonetheless, we can use any of the energy models presented in Section 2 to calculate the point-to-point energy requirements in Δe given the fact that the upper bound on extra mass is known (the number of passengers $u[i]$ is at most C). In the next section, we measure the impacts of each model on the planned routes.

We now explain our charging constraints. To model charging profiles without linear piece-wise approximation, we map each profile into an array indexed by time. Figure 4 (Left) depicts how we discretise a sample charging profile based on a time unit. In our model, $e^*[\tau]$ represents the amount of energy charged in a fully discharged battery if the EV has been in the charging station for τ units of time. Since EVs are not allowed to have negative energy levels (or we always have $0 \le e^*[\tau]$), we use τ as an offset for charging time t_c. This means if the EV arrives at a charging point with energy $e_1^*[\tau_1]$ and departs with energy $e_2^*[\tau_2]$, we have $t_c = \tau_2 - \tau_1$ as the charging time. Therefore, for every visited charging node i we have

$$e^*[\tau[i]] \le e[i] < e^*[\tau[i] + 1] \qquad i \in charger \quad \text{and} \quad \tau[i] \in [0, T_c) \tag{10}$$
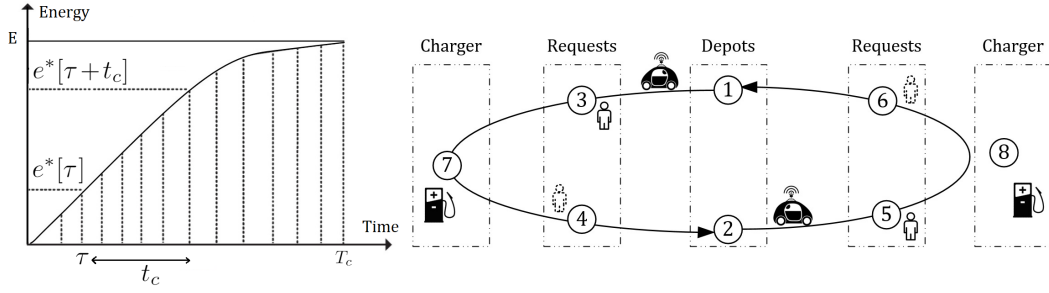
Figure 4 Left: Charging profile, Right: Sample trips using the `subcircuit` constraint.

where $e[i]$ is the EV energy at arrival and $\tau[i]$ is the corresponding time offset for charger node i. T_c is also the maximum charging time to get charged for the full energy capacity E. Note that the constraint above looks up the closest (mapped) value to $e[i]$ such that the actual charging time always falls in the interval $[\tau, \tau + 1)$. This means the discretisation approach may lead to overestimating the charging time by at most one unit of time. Now, given $e^*[\tau + t_c]$ as the energy of the EV after visiting a charging node, we can set a constraint on the energy of the EV when it arrives at a successor node via a charging node.

$$e[j] = e^*[\tau[i] + t_c[i]] - \Delta e[i, j, k] \qquad i \in charger \quad \text{and} \quad j = succ[i] \quad \text{and} \quad k = u[i] \quad (11)$$

The constraint above ensures that the energy consumption is appropriately tracked after every charging visit, but we need to make sure that the charging time is also incorporated in the total trip time. To this end, we first limit the charging time per charging node by

$$0 \le t_c[i] \le T_c - \tau[i] \qquad i \in charger \quad (12)$$

where t_c is the charging time and T_c is the maximum charging time (time needed to get charged from 0 to 100% energy level). The constraint above also enforces that discharging in charging stations is not allowed as the charging time is always non-negative.

Now we finally define the lower arrival time to successor nodes via charging nodes to be

$$t[j] \ge t[i] + t_c[i] + t_s[i] + \Delta t[i, j] \qquad i \in charger \quad \text{and} \quad j = succ[i] \quad (13)$$

where $t[i]$ is the time the EV arrives at the charging point and $t[j]$ is the time it is at the successor node. Furthermore, t_s is the service time spent at the charging node. Note that since different charging technologies have different charging profiles, we store our mapped energy values in a 2-dimensional array where the other dimension determines the charging type, i.e., we have $e^*[\tau[i], \epsilon[i]]$ where $\epsilon[i]$ would be the charging type of node i. Each charging node in our PDP model can handle one charging visit at a time. If some or all charger locations can handle more than one charging visit at a time, we need to create multiple charging nodes for these charging locations, each capable of handling one visit. In this case, the model may need additional constraints for charger scheduling.

Finally, the objective is to minimise the total driving time and charging time.

$$Minimise \quad (\sum_{i \in N} \Delta t[i, succ[i]] + \sum_{i \in char} t_c[i]) \quad (14)$$

4   Benchmark Setup

Transport models for EVs require accurate energy estimates on the underlying point-to-point paths. In order to examine our PDP model under realistic scenarios, a set of instances with all the energy measures (point-to-pint energy requirements for different energy models) is required. To this end, following the strategy used in [4], we use the GPS traces from Uber Technologies Inc.[3] to extract random realistic trips. The data file includes the GPS logs of more than 20,000 ride-sharing trips in San Francisco (CA, USA) over one week. Furthermore, choosing San Francisco as the test city allows us to better investigate the significance of gradient as one of the main parameters of vehicle dynamics.

Previous works on routing problems for EVs have used (partially) synthetic datasets and/or simplified energy models. For example, the well-known Solomon vehicle routing benchmark [17] is a commonly used synthetic dataset that has been adapted to EVs in [10, 16]. Since parameters in synthetic datasets are not fully realistic, they cannot perfectly reflect all the real challenges in EVs, especially energy-related parameters such as non-linear charging profiles and vehicle dynamics. Given the importance of energy parameters in EV routing problems, some recent studies have tried to establish more realistic datasets by respecting the relationships between distance, time and energy [9, 13, 4]. Nonetheless, these datasets are still not complete enough to be used in our complete energy-based PDP model.

We now explain our strategy to generate random test cases from the Uber ride-sharing dataset. Each line of the data file is in the following format:

<center><trip ID> <timestamp> <latitude> <longitude></center>

Every trip ID in the data file can be found in two lines, one for pickup and another for the corresponding drop-off. We rebuild every point-to-point transport demand using the pickup and drop-off locations (latitude, longitude). The travelled distance of trip IDs ranges from 100m to 15km, but to better analyse the energy matters in the PDP with EVs, we randomly pick trips of 8km and longer. The Uber GPS log file contains all the necessary data for traditional route planning models such as time and transport origin and destination, but part of the input data to our system model still needs to be determined with extra considerations.

Time windows.   For each selected trip ID, we pick the timestamp of the pickup entry (the one with an earlier timestamp) as the desired pickup time. We then consider a 15-minute time window for every transport demand at pickup. As an example, if the actual pickup time of a transport request in the data file is t_{pu}, its corresponding time window is considered to be $[t_{pu} - 7.5min, t_{pu} + 7.5min]$. We set our time scaling factor λ to 1.5, meaning that the trip time of each individual transport request is at most 50% longer than its direct path. We also set 30 seconds as service time for every non-depot node.

Extra stop locations.   We assume the EVs' depot to be a location in the city area of San Francisco. We also choose five charging locations from an online service[4]: three normal and two fast-charge points (one of the normal chargers at the depot). In addition, EVs are expected to return to the depot after serving transport demands. To prevent frequent charging detours, we limit EVs to at most one charging visit in each trip.

---

[3] `https://github.com/dima42/uber-gps-analysis/tree/master/gpsdata`
[4] `https://www.plugshare.com/`
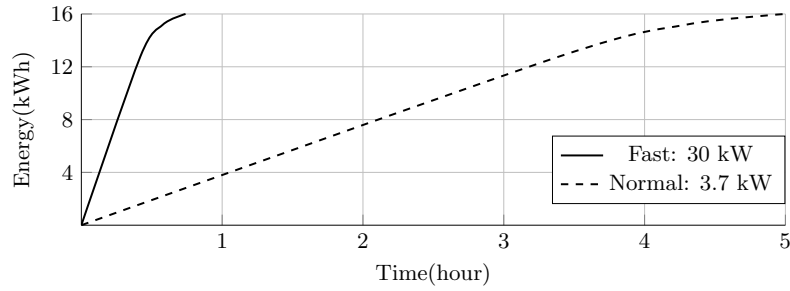
■ **Figure 5** Normal and Fast charge profiles for *Peugeot iOn* with 16 kWh battery capacity.

Test EV.   We choose our test EV to be the *Peugeot iOn*, one of the commonly used EVs in the literature with a vehicle capacity of four passengers and an energy capacity of 16 kWh [11]. We consider 75 kg for each passenger's weight[5] in our energy calculation. Figure 5 depicts the actual non-linear charging profiles of two charging technologies (normal and fast) available for the test vehicle of this study with the maximum charging time of five hours.

Energy coefficients.   For the test EV of this study, we used an advanced (open source) EV simulator called ADVISOR(ADvance VehIcle SimulatOR)[6] to learn our energy models and set coefficients α_i and β_i in Section 2. This software is developed on the engineering platform MATLAB and is enriched with complete powertrain models. The model of each component (such as the battery, electric machine, etc.) incorporates parameters such as all detailed equations of vehicle dynamics, temperature profiles, efficiency maps, auxiliary loads or even warm/cold start [1, 12]. Therefore, the selected simulator provides more accurate estimates on energy requirements of EVs under a variety of realistic scenarios, such as transporting different numbers of passengers on a road with a non-zero slope).

EV considerations.   We assume that our EVs can use their full energy capacity, i.e., their energy level can be 0–100% and there is no limit for them at the end of the trips. Moreover, we assume that our EVs start their trips with 100% initial energy level.

Underlying graph.   We extract the San Francisco road network from OpenStreetMap using the Python package OSMnx [3] and enrich the graph edges of the road network with elevation and speed data using the *Bing*, *Mapbox*, *Here* and *TomTom* APIs[7].

Point-to-point paths.   Given the road network of San Francisco as our underlying graph, we propose two types of paths for our experimental analysis:
1. *Shortest path:* for our base approach, we consider all point-to-point paths in our problem to be shortest path. For this purpose, we compute our first set of paths using Dijkstra's algorithm [6] for any (origin,destination) pair in the instance.
2. *Energy-efficient path:* for our second approach, we optimise all point-to-point paths for their energy consumption, that is, instead of solving the underlying graph for *time*, we are interested in a path that offers the lowest energy consumption. As the energy requirement of links of the graph can be negative (in negative slopes), we use an adapted version of the Bellman-Ford algorithm [2, 7] to calculate point-to-point energy-optimal paths. Our adapted version uses the most accurate energy model presented in Section 2 (Eq. (1)) and takes the battery limits into account.

---

[5] Based on European Directive 95/48/EC
[6] `http://adv-vehicle-sim.sourceforge.net/`
[7] `www.bing.com; www.mapbox.com; developer.here.com; developer.tomtom.com`

Time and energy arrays. The additional required information includes the time (Δt array) and energy (Δe array) requirements of all point-to-point paths. So far we have obtained two sets of paths for each problem instance. In the next step, we need to determine our time and energy arrays (resp. Δt and Δe) for each set. To this end, we take the resulting paths and compute their time simply via converting the *distance* attribute of the links of the paths to time using an average speed. For their energy requirement, we use all of our four energy models presented in Section 2 and generate four energy arrays for each set of paths. Note that we do not change the optimum paths in each set, but we recalculate the energy requirement of the paths each time with a different approach. Creating separate energy arrays allows us to better investigate the impacts of vehicle dynamics on our planned routes. We also set time and energy units to 10 Wh and 30 seconds respectively.

Instance format. Each instance is presented in the format of $< uv - t - n >$ where v is the number of EVs, t is the number of transport requests and n is the instance variant. For example, the instance $< u1 - 10 - 2 >$ is our second instance with 10 transport requests and one vehicle. We arbitrarily keep the number of the transport requests small. As finding the optimal solution to each instance is necessary for our energy analysis, we avoid generating very large and difficult instances. Each instance consists of the required input for our energy-based PDP model such as time windows, utilisation at each pickup, time and energy arrays, charger profiles and energy/time upper bounds. Our instances are publicly available [8].

5 Results and Discussion

We developed our model in MiniZinc and and evaluated that using the CP solver Chuffed [5] as the back-end optimiser with the *free search* flag. We found MiniZinc MIP solvers slower for our CP model over the instances. For each scenario of point-to-point paths, we solved all of the instances to optimality using different energy models (resp. energy arrays). The proposed solver could solve our difficult instances with 20 demands, five chargers and two vehicles in a 90-minute timeout on a machine with an Intel Core i7-10850H running at 2.7 GHz and with 32 GB of RAM. Regarding the computational effort, we found handling charger nodes the main solving challenge as the charging time can be even larger than the trip time (five hours for normal chargers). As we will see later in this section, the solver rarely plans trips that include visits to normal chargers. As a further optimisation, we could reduce the runtime by introducing a subset of charger nodes in multiple runs of the model to improve the objective upper bound. For example, by removing the normal slow chargers from the list of stops we could solve the instances much faster (usually in less than five minutes). We also found the problem much more challenging for the solver with increased number of transport requests and vehicles. The standard solver was unable to optimally solve our larger instance with 30 demands and three vehicles in the time limit. It is worth highlighting that we did not notice a major difference in the runtime of the models with mass consideration (models without mass consideration were solved slightly faster).

Tables 3 and 4 present the results of solving the PDP for the designed instances of this study in two different scenarios. Table 3 shows the results for the first scenario with shortest point-to-point paths, and Table 4 presents the results for the second scenario with energy-optimum paths as an alternative. In the both tables, attribute E_b denotes that the transport model has been evaluated with the *basic* energy model for point-to-point energy calculations.

---

[8] https://bitbucket.org/s-ahmadi

Similarly, E_g and E_{gv} indicate the use of additional parameters *gradient* and *speed* in the energy models. The results are shown without (left columns) and with (right columns) taking extra mass into account. Finally, the results for our full energy model are indicated with E_{gv}^m with all parameters considered. We again emphasise that the point-to-point paths in each scenario are the same for all of the models and only the energy calculation method is different. In the energy-efficient paths scenario, the point-to-point paths were pre-computed based on our full energy model E_{gv}^m. Our studied parameters consist of the value of the total driving time (t_{dr}), total charging time (t_{ch}), energy consumed while driving (e_{dr}), energy charged at charging nodes (e_{ch}), type of chargers used (ϵ), the ratio of the difference in routes ($\phi_r = \Delta R/R_b$) with the routes of E_b as the base, and the energy miscalculation ratio $\phi_e = \Delta E/E_{gv}^m$ with E_{gv}^m as the base (complete) energy model. We calculate the ratio $\Delta R/R_b$ by comparing the optimum *Successor* array against that of the base case obtained for E_b. In addition, we define the energy error ΔE to be the difference between energy values in E_{gv}^m and other models (E_b, E_g etc.).

We start our analysis with the results shown in Table 3. According to the route difference ratio, routes may vary up to 20% if we do not opt for the basic energy model in point-to-point energy calculations. Furthermore, we can see that in all cases, the energy consumption of tours increases when more accurate energy models are considered for our energy array. This means the basic energy model is the least accurate model, underestimating the trips' energy requirement in all of the instances. Nonetheless, the table shows that the mass-based energy model E_b^m is still not as accurate as the gradient-based models E_g or E_{gv} with both mass and speed added. Therefore, we can conclude that the gradient in E_g has more impact on energy consumption than mass in E_b^m.

The results in Table 3 show that taking driving patterns into consideration (models E_{gv} and E_{gv}^m) further increases the trips' energy requirement. The main reason is that there are generally more low-speed links on inner-city trips than other speed profiles, and low-speed links require more energy than medium or high-speed profiles (see energy coefficients in Table 1). This inefficiency is technically rooted in energy loss via frequent stop-go patterns in inner-city trips and little energy recuperation at low speeds.

In several cases, we see that serving transport requests with more accurate energy models is only feasible if a charging detour is planned. In other words, routes planned based on less accurate energy models can potentially be infeasible in reality as they might not consider any charging detour at critical energy levels. In the *u1-10-1* and *u2-20-3* instances, for example, we have a case where only our full energy model E_{gv}^m plans a route with a charging detour while other models assume the initial energy of the EVs is sufficient for the entire trip. These instances highlight another important observation. Although we already concluded that the gradient and driving speed have more impact on optimal routes than mass, as our full model E_{gv}^m considers all parameters including extra mass, we can see that neglecting mass may lead to planning infeasible routes even with relatively accurate energy estimates via E_{gv}.

Our next observation is that the objective value ($t_{dr} + t_{ch}$) changes when a different route is planned (non-zero ϕ_r) to meet the energy limits and also every time the models introduce a charging detour to the planned routes. For example, a 10.5-minute charging time is required to fast charge the EV for 5.19 kWh in instance *u1-10-5* using our full model E_{gv}^m. Note that the basic model E_b in this instance also plans a charging detour, but its estimated charging time is almost half (4.5-minute) of the charging time planned via E_{gv}^m. This is mainly because of around 3.1 kWh underestimation of energy in E_b. This significant difference in charging times means that having a charging visit in our plan does not necessarily guarantee the feasibility of trips. Therefore, having an accurate energy model is also vital for the correct calculation of charging times.

Table 4 shows the results when energy-optimum paths are used for the pre-computation of the time and energy arrays. A quick look over the values reminds us of the pattern we observed in Table 3 for time and energy values. We see larger time and energy values when more accurate models are employed in our PDP transport system, but there are some meaningful differences when we compare them with the results in Table 3. Firstly, energy efficient paths result in longer trips (larger objective values). This is mainly because of the fact that energy-efficient point-to-point paths are normally longer than shortest paths. Secondly, compared to the routes with shortest paths (Table 3), routes planned with energy-efficient paths using the E_b or E_b^m model consume more energy. The reason is, again, related to having longer paths and consequently larger energy values for point-to-point paths via simple distance based energy models. Nonetheless, if we compare the results of the tables for E_g and E_{gv}, the case is reversed and the impact of the gradient is revealed. Although we have not defined any explicit energy objective for our PDP, we can see that energy-optimum paths are actually contributing to lower energy consumption in all of our instances via our more accurate models E_g and E_{gv}, while making sure that all the transport requests have also been served. We can see the same pattern for the gradient and speed-based models with extra mass consideration, i.e., E_g^m and E_{gv}^m.

The results in Table 4 also show that energy-optimum paths via the E_g and E_{gv} models (and their mass-added variants) also contribute to less charging time in our instances. Interestingly, there are even several cases where no charging visit is required if we opt for energy optimum paths over traditional shortest paths. In instance *u2-20-5* using the accurate model E_{gv}^m, for example, we can avoid a charging detour for 2.91 kWh extra energy in six minutes. Comparing the time and energy values of the instance for E_{gv}^m from the tables, we notice that we can save 1.27 kWh by planing a route that is even 0.5 minutes faster than the traditional time-efficient route with a charging detour. It is worth mentioning that there is always a trade-off between total trip time and energy consumption. We can see that trips planned using the efficient paths can be more energy-efficient and at the same time slightly longer than trips obtained by shortest paths on average. Nevertheless, we can deduce that fewer/shorter charging visits are required via more accurate models if energy optimum paths are chosen and all transport request are satisfied.

The results in both tables show that the energy error ratio in an instance can be as big as 16.3% when using the basic energy model E_b. For our gradient and speed-based energy models E_g and E_{gv} the error ratios are at most 8.0% and 4.9% respectively over the instances. We also compared the average underestimation of energy in both tables for the instances with no change in the planned route (zero ϕ_r), e.g. instance *u1-10-6*. For this instance, we have a maximum error ratio of 11.0% in Table 3 but a smaller error in Table 4 for energy efficient paths (7.7% for model E_b). We see that the energy error ratio of using the shortest path is about 40% larger than that of using the energy-optimum path.

Tables 3, 4 also show the charger type used at any charging visit. According to the results, although we have more normal chargers than fast chargers in our instances, normal chargers are barely used in our PDP routes and fast chargers are preferred in almost all of the charging detours. In particular, only one of the charging visits in each scenario (Tables 3,4) uses the normal type. The likely reason for this choice is our objective to minimise the total travel time (including charging time) knowing that normal chargers are at least four times slower than fast chargers (see Figure 5). Therefore, slow chargers with low energy rates can potentially be removed from the charging nodes of transport models with EVs, reducing the routing complexity and runtime.

■ **Table 3** Experiment results using the shortest point-to-point paths, for every energy model (E.) with and without mass consideration in Δe. The results include driving time (t_{dr}) in minutes, charge time (t_{ch}) in minutes, energy consumed while driving (e_{dr}) in kWh, energy recharged at charger points (e_{ch}) in kWh, charger type used (ϵ) from {normal/fast}, route difference ratio (ϕ_r) and energy error (ϕ_e).

Instance	E.	t_{dr} min	t_{ch} min	e_{dr} kWh	e_{ch} kWh	ϵ n,f	ϕ_r %	ϕ_e %	E.	t_{dr} min	t_{ch} min	e_{dr} kWh	e_{ch} kWh	ϵ n,f	ϕ_r %	ϕ_e %
							Without Mass Consideration							With Mass Consideration		
u1-10-1	E_b	153.5	0.0	13.89	0.00	-	-	14.2	E_b^m	153.5	0.0	14.24	0.00	-	0.0	12.0
	E_g	153.5	0.0	15.11	0.00	-	0.0	6.7	E_g^m	153.5	0.0	15.67	0.00	-	0.0	3.2
	E_{gv}	153.5	0.0	15.60	0.00	-	0.0	3.6	E_{gv}^m	153.0	1.0	16.19	0.36	f	7.7	-
u1-10-2	E_b	160.5	0.0	14.59	0.00	-	-	13.9	E_b^m	160.5	0.0	14.88	0.00	-	7.7	12.2
	E_g	160.5	0.0	15.65	0.00	-	11.5	7.7	E_g^m	161.0	1.5	16.27	0.38	f	15.4	4.0
	E_{gv}	161.5	1.5	16.38	0.60	f	15.4	3.4	E_{gv}^m	161.5	2.5	16.95	1.06	f	15.4	-
u1-10-3	E_b	161.5	0.0	14.63	0.00	-	-	15.3	E_b^m	161.5	0.0	15.04	0.00	-	0.0	12.9
	E_g	161.5	0.0	15.93	0.00	-	0.0	7.8	E_g^m	163.5	2.0	16.78	0.83	f	7.7	2.8
	E_{gv}	163.5	1.5	16.59	0.76	f	7.7	3.9	E_{gv}^m	163.5	3.0	17.27	1.34	f	7.7	-
u1-10-4	E_b	173.0	0.0	15.61	0.00	-	-	14.2	E_b^m	173.0	0.0	15.98	0.00	-	0.0	12.2
	E_g	173.0	2.5	17.01	1.16	f	7.7	6.5	E_g^m	173.0	3.5	17.51	1.53	f	7.7	3.7
	E_{gv}	173.0	3.5	17.68	1.68	f	7.7	2.8	E_{gv}^m	173.0	5.0	18.19	2.31	f	7.7	-
u1-10-5	E_b	198.5	4.5	18.02	2.27	f	-	14.7	E_b^m	198.5	5.5	18.42	2.66	f	0.0	12.8
	E_g	198.5	8.5	19.94	4.03	f	0.0	5.6	E_g^m	198.5	10.0	20.42	4.42	f	0.0	3.3
	E_{gv}	198.5	10.0	20.53	4.55	f	0.0	2.8	E_{gv}^m	199.5	10.5	21.12	5.19	f	11.5	-
u1-10-6	E_b	205.0	5.5	18.48	2.67	f	-	11.0	E_b^m	205.0	6.5	18.90	3.08	f	0.0	9.0
	E_g	205.0	7.0	19.39	3.43	f	0.0	6.7	E_g^m	205.0	8.0	19.88	3.88	f	0.0	4.3
	E_{gv}	205.0	8.5	20.23	4.28	f	0.0	2.6	E_{gv}^m	205.0	10.0	20.77	5.00	f	0.0	-
u1-14-1	E_b	173.0	0.0	15.74	0.00	-	-	15.9	E_b^m	175.5	1.5	16.54	0.63	f	20.6	11.6
	E_g	175.5	3.0	17.23	1.48	f	14.7	7.9	E_g^m	175.5	5.0	18.11	2.35	f	14.7	3.2
	E_{gv}	175.5	4.0	17.81	1.90	f	14.7	4.8	E_{gv}^m	175.5	5.5	18.71	2.78	f	5.8	-
u2-20-1	E_b	283.5	0.0	25.82	0.00	-	-	16.3	E_b^m	283.5	0.0	26.58	0.00	-	0.0	13.7
	E_g	283.5	0.0	28.78	0.00	-	0.0	6.6	E_g^m	284.0	0.0	30.10	0.00	-	14.9	2.3
	E_{gv}	283.5	0.0	29.54	0.00	-	0.0	4.1	E_{gv}^m	284.5	0.0	30.81	0.00	-	6.4	-
u2-20-2	E_b	290.5	0.0	26.16	0.00	-	-	14.5	E_b^m	290.5	0.0	26.93	0.00	-	4.3	12.0
	E_g	290.5	0.0	28.68	0.00	-	0.0	6.3	E_g^m	290.5	0.0	29.67	0.00	-	4.3	3.1
	E_{gv}	290.5	0.0	29.61	0.00	-	4.3	3.3	E_{gv}^m	290.5	0.0	30.61	0.00	-	0.0	-
u2-20-3	E_b	301.5	0.0	27.50	0.00	-	-	14.5	E_b^m	301.5	0.0	28.22	0.00	-	0.0	12.3
	E_g	301.5	0.0	30.39	0.00	-	0.0	5.6	E_g^m	301.5	0.0	31.58	0.00	-	0.0	1.8
	E_{gv}	301.5	0.0	31.21	0.00	-	0.0	3.0	E_{gv}^m	302.0	3.0	32.18	0.68	f	12.8	-
u2-20-4	E_b	303.5	0.0	27.54	0.00	-	-	14.5	E_b^m	303.5	0.0	28.36	0.00	-	0.0	13.5
	E_g	304.5	0.0	30.70	0.00	-	14.9	6.3	E_g^m	305.0	0.0	31.91	0.00	-	4.3	2.6
	E_{gv}	305.0	0.0	31.59	0.00	-	8.5	3.6	E_{gv}^m	303.5	3.5	32.78	1.68	f	14.9	-
u2-20-5	E_b	308.5	0.0	27.98	0.00	-	-	15.7	E_b^m	308.5	0.0	28.71	0.00	-	0.0	12.5
	E_g	308.5	0.0	30.74	0.00	-	0.0	6.3	E_g^m	309.0	1.0	31.95	0.07	n	4.3	2.7
	E_{gv}	308.5	0.0	31.47	0.00	-	0.0	4.1	E_{gv}^m	310.5	6.0	32.82	2.91	f	17.0	-
u2-20-6	E_b	322.5	0.0	29.06	0.00	-	-	15.6	E_b^m	322.5	0.0	28.36	0.00	-	0.0	13.5
	E_g	323.5	0.0	31.73	0.00	-	12.8	7.8	E_g^m	324.0	2.5	33.02	1.23	f	19.1	4.1
	E_{gv}	324.0	2.5	32.84	1.18	f	19.1	4.6	E_{gv}^m	324.5	5.5	34.43	2.47	f	14.9	-

■ **Table 4** Experiment results using the lowest energy point-to-point paths, for every energy model (E.) with and without mass consideration in Δe. The results include driving time (t_{dr}) in minutes, charge time (t_{ch}) in minutes, energy consumed while driving (e_{dr}) in kWh, energy recharged at charger points (e_{ch}) in kWh, charger type used (ϵ) from {normal/fast}, route difference ratio (ϕ_r) and energy error (ϕ_e).

Instance	E.	t_{dr} min	t_{ch} min	e_{dr} kWh	e_{ch} kWh	ϵ n,f	ϕ_r %	ϕ_e %	E.	t_{dr} min	t_{ch} min	e_{dr} kWh	e_{ch} kWh	ϵ n,f	ϕ_r %	ϕ_e %
				Without Mass Consideration								With Mass Consideration				
u1-10-1	E_b	155.5	0.0	14.02	0.00	-	-	11.7	E_b^m	155.5	0.0	14.40	0.00	-	0.0	9.3
	E_g	155.5	0.0	14.74	0.00	-	0.0	7.1	E_g^m	155.5	0.0	15.27	0.00	-	0.0	3.8
	E_{gv}	155.5	0.0	15.31	0.00	-	0.0	3.5	E_{gv}^m	155.5	0.0	15.87	0.00	-	0.0	-
u1-10-2	E_b	162.5	0.0	14.74	0.00	-	-	12.0	E_b^m	162.5	0.0	15.07	0.00	-	0.0	10.0
	E_g	162.5	0.0	15.41	0.00	-	0.0	8.0	E_g^m	162.5	0.0	15.94	0.00	-	0.0	4.8
	E_{gv}	162.5	0.5	16.02	0.03	n	7.7	4.3	E_{gv}^m	163.5	2.0	16.74	0.86	f	7.7	-
u1-10-3	E_b	162.0	0.0	14.68	0.00	-	-	14.45	E_b^m	162.0	0.0	15.11	0.00	-	0.0	11.9
	E_g	162.0	0.0	15.79	0.00	-	0.0	8.0	E_g^m	164.0	1.5	16.61	0.73	f	7.7	3.2
	E_{gv}	164.0	1.5	16.56	0.75	f	19.2	3.5	E_{gv}^m	164.0	2.5	17.16	1.27	f	7.7	-
u1-10-4	E_b	176.0	0.0	15.86	0.00	-	-	10.2	E_b^m	176.5	1.0	16.29	0.37	-	7.7	7.8
	E_g	176.5	1.5	16.55	0.73	f	7.7	6.3	E_g^m	176.5	2.5	16.99	1.07	f	7.7	3.8
	E_{gv}	176.5	3.0	17.22	1.46	f	7.7	2.5	E_{gv}^m	176.5	3.5	17.67	1.76	f	7.7	-
u1-10-5	E_b	201.5	4.5	18.11	2.20	f	-	11.3	E_b^m	201.5	5.0	18.51	2.54	f	0.0	9.3
	E_g	201.5	7.0	19.26	3.40	f	11.5	5.6	E_g^m	201.5	8.0	19.75	3.84	f	11.5	3.2
	E_{gv}	201.5	8.0	19.89	4.05	f	11.5	2.5	E_{gv}^m	201.5	9.0	20.41	4.51	f	11.5	-
u1-10-6	E_b	208.0	6.0	18.83	2.84	f	-	7.7	E_b^m	208.0	6.5	19.25	3.25	f	0.0	5.7
	E_g	208.0	7.0	19.31	3.37	f	0.0	5.4	E_g^m	208.0	7.5	19.78	3.81	f	0.0	3.1
	E_{gv}	208.0	8.0	19.90	4.05	f	0.0	2.5	E_{gv}^m	208.0	9.0	20.41	4.51	f	0.0	-
u1-14-1	E_b	177.5	1.0	16.04	0.05	-	-	12.4	E_b^m	179.5	2.0	16.80	0.97	f	17.6	8.2
	E_g	179.5	2.5	16.96	1.05	f	8.8	7.4	E_g^m	179.5	4.0	17.77	1.90	f	17.6	2.9
	E_{gv}	179.5	3.5	17.41	1.60	f	17.6	4.9	E_{gv}^m	179.5	5.0	18.31	2.50	f	8.8	-
u2-20-1	E_b	286.5	0.0	25.99	0.00	-	-	13.7	E_b^m	286.5	0.00	26.77	0.00	-	0.0	11.1
	E_g	286.5	0.0	28.02	0.00	-	0.0	7.0	E_g^m	286.5	0.00	29.06	0.00	-	0.0	3.5
	E_{gv}	286.5	0.0	28.94	0.00	-	0.0	3.9	E_{gv}^m	287.5	0.00	30.12	0.00	-	6.4	-
u2-20-2	E_b	291.5	0.0	26.33	0.00	-	-	12.4	E_b^m	292.5	0.0	27.20	0.0	-	4.3	9.5
	E_g	293.5	0.0	28.00	0.00	-	8.5	6.8	E_g^m	293.5	0.0	28.92	0.0	-	8.5	3.7
	E_{gv}	293.5	0.0	29.04	0.00	-	8.5	3.3	E_{gv}^m	293.5	0.0	30.04	0.0	-	8.5	-
u2-20-3	E_b	305.5	0.0	27.86	0.00	-	-	11.6	E_b^m	305.5	0.0	28.58	0.00	-	0.0	9.4
	E_g	305.5	0.0	29.37	0.00	-	0.0	6.9	E_g^m	305.5	0.0	30.45	0.00	-	0.0	3.4
	E_{gv}	305.5	0.0	30.37	0.00	-	0.0	3.7	E_{gv}^m	306.0	0.0	31.53	0.00	-	8.5	-
u2-20-4	E_b	304.5	0.0	27.59	0.00	-	-	13.9	E_b^m	304.5	0.0	28.44	0.00	-	0.0	11.2
	E_g	304.5	0.0	29.72	0.00	-	0.0	7.2	E_g^m	304.5	1.5	30.94	0.61	f	8.5	3.4
	E_{gv}	304.5	1.0	30.75	0.29	f	8.5	4.0	E_{gv}^m	304.5	2.5	32.03	1.11	f	8.5	-
u2-20-5	E_b	307.0	0.0	27.81	0.00	-	-	11.9	E_b^m	307.0	0.0	28.60	0.00	-	0.0	9.4
	E_g	307.0	0.0	29.25	0.00	-	0.0	7.3	E_g^m	309.5	0.0	30.48	0.00	-	8.5	3.4
	E_{gv}	309.5	0.0	30.44	0.00	-	8.5	3.5	E_{gv}^m	310.0	0.0	31.55	0.00	-	10.6	-
u2-20-6	E_b	325.5	0.0	29.42	0.00	-	-	12.9	E_b^m	325.5	0.0	30.26	0.00	-	0.0	10.4
	E_g	326.5	0.0	31.32	0.00	-	8.5	7.3	E_g^m	326.0	2.0	32.59	0.80	f	14.9	3.5
	E_{gv}	326.5	1.5	32.42	0.61	f	14.9	4.0	E_{gv}^m	327.5	5.0	33.78	2.45	f	21.3	-

6 Conclusion

This paper investigates the impacts of vehicle dynamics on routing problems with Electric Vehicles (EVs), particularly in the Pickup-and-Delivery Problem (PDP). We developed a model for the PDP based on six different energy calculation methods that considers parameters of vehicle dynamics to varying degrees. The selected parameters are road gradient, extra mass and driving patterns (speed profiles). We also developed a complete PDP system model with charging and energy constrains and evaluated our underlying energy models under a set of adapted realistic instances. The results indicate that the energy requirement of routes planned for EVs can be underestimated by up to 16.3% in our instances if the fundamental parameters of gradient, speed and mass are ignored in the energy calculations. Although adding the mass metric into the energy calculation increases the model complexity, the results of this study show that ignoring mass from the energy calculation of EVs can potentially lead to infeasible trips with insufficient energy to complete the planned trip. Comparing the impacts of parameters on routes' energy attributes, we can see that gradient and speed make a greater contribution to the actual energy requirement of routes than mass in our experiment. We also investigate an alternative scenario for point-to-point paths in the PDP by optimising underlying paths for their energy consumption. The results of experiments on our instances show that choosing energy-optimum paths instead of traditional shortest paths can make the planned trips more efficient in terms of energy, but slightly longer in term of time. Nonetheless, trips planned with our alternative scenario showed better energy efficiency and require less/shorter charging visits.

The use of a high-level, constraint-based modelling system like MiniZinc allowed us to experiment with these different energy models without creating new dedicated solving approaches. The results from our experiments show that a significant investment in such new algorithms may not only be useful, but crucial in order to ensure valid and efficient vehicle routing with EVs.

Future work could look at integrating the energy models of this study with other real-world routing problems for EVs, for example trip planning period. For PDP, an interesting direction is developing/adapting appropriate heuristics for our complete energy-based model, as adding mass to the calculation increases the complexity and runtime.

References

1. Saman Ahmadi, SMT Bathaee, and Amir H Hosseinpour. Improving fuel economy and performance of a fuel-cell hybrid electric vehicle (fuel-cell, battery, and ultra-capacitor) using optimized energy management strategy. *Energy Conversion and Management*, 160:74–84, 2018.

2. Richard Bellman. On a routing problem. *Quarterly of applied mathematics*, 16(1):87–90, 1958.

3. Geoff Boeing. Osmnx: New methods for acquiring, constructing, analyzing, and visualizing complex street networks. *Comput. Environ. Urban Syst.*, 65:126–139, 2017. `doi:10.1016/j.compenvurbsys.2017.05.004`.

4. Claudia Bongiovanni, Mor Kaspi, and Nikolas Geroliminis. The electric autonomous dial-a-ride problem. *Transportation Research Part B: Methodological*, 122:436–456, 2019.

5. Geoffrey Chu. *Improving Combinatorial Optimization*. PhD thesis, Department of Computing and Information Systems, University of Melbourne, 2011.

6. Edsger W. Dijkstra. A note on two problems in connexion with graphs. *Numerische Mathematik*, 1:269–271, 1959. `doi:10.1007/BF01386390`.

7. Lester R Ford Jr. Network flow theory. Technical report, Rand Corp Santa Monica Ca, 1956.

8   Dominik Goeke. *Emerging Trends in Logistics: New Models and Algorithms for Vehicle Routing.* PhD thesis, Department of Business and Economics at the University of Kaiserslautern, 2018.

9   Dominik Goeke and Michael Schneider. Routing a mixed fleet of electric and conventional vehicles. *Eur. J. Oper. Res.*, 245(1):81–99, 2015. `doi:10.1016/j.ejor.2015.01.049`.

10   Merve Keskin and Bülent Çatay. A matheuristic method for the electric vehicle routing problem with time windows and fast chargers. *Comput. Oper. Res.*, 100:172–188, 2018. `doi:10.1016/j.cor.2018.06.019`.

11   Çagri Koç, Ola Jabali, Jorge E. Mendoza, and Gilbert Laporte. The electric vehicle routing problem with shared charging stations. *Int. Trans. Oper. Res.*, 26(4):1211–1243, 2019. `doi:10.1111/itor.12620`.

12   Tony Markel, Aaron Brooker, T Hendricks, V Johnson, Kenneth Kelly, Bill Kramer, Michael O'Keefe, Sam Sprik, and Keith Wipke. Advisor: a systems analysis tool for advanced vehicle modeling. *Journal of power sources*, 110(2):255–266, 2002.

13   Alejandro Montoya, Christelle Guéret, Jorge E. Mendoza, and Juan G. Villegas. The electric vehicle routing problem with nonlinear charging function. *Transportation Research Part B: Methodological*, 103:87–110, 2017. Green Urban Transportation. `doi:10.1016/j.trb.2017.02.004`.

14   Nicholas Nethercote, Peter J. Stuckey, Ralph Becket, Sebastian Brand, Gregory J. Duck, and Guido Tack. Minizinc: Towards a standard CP modelling language. In Christian Bessiere, editor, *Principles and Practice of Constraint Programming - CP 2007, 13th International Conference, CP 2007, Providence, RI, USA, September 23-27, 2007, Proceedings*, volume 4741 of *Lecture Notes in Computer Science*, pages 529–543. Springer, 2007. `doi:10.1007/978-3-540-74970-7_38`.

15   Samuel Pelletier, Ola Jabali, and Gilbert Laporte. Charge scheduling for electric freight vehicles. *Transportation Research Part B: Methodological*, 115:246–269, 2018. `doi:10.1016/j.trb.2018.07.010`.

16   Michael Schneider, Andreas Stenger, and Dominik Goeke. The electric vehicle-routing problem with time windows and recharging stations. *Transp. Sci.*, 48(4):500–520, 2014. `doi:10.1287/trsc.2013.0490`.

17   Marius M. Solomon. Algorithms for the vehicle routing and scheduling problems with time window constraints. *Oper. Res.*, 35(2):254–265, 1987. `doi:10.1287/opre.35.2.254`.

18   Paolo Toth and Daniele Vigo. *Vehicle Routing.* Society for Industrial and Applied Mathematics, Philadelphia, PA, 2014. `doi:10.1137/1.9781611973594`.

19   Hao Wang and Ruey Long Cheu. Operations of a taxi fleet for advance reservations using electric vehicles and charging stations. *Transportation Research Record*, 2352(1):1–10, 2013. `doi:10.3141/2352-01`.